

## A PERMEABILITY MODEL OF PACKED PARTICLES MATERIAL BASED ON 2-D FRACTAL GRADATION SPECTRUM

by

**Fan ZUO<sup>a</sup>, Junqing LIU<sup>b</sup>, Meng LI<sup>a</sup>, and Chao LIU<sup>a,b\*</sup>**

<sup>a</sup> School of Civil Engineering, Xi'an University of Architecture and Technology, Xi'an, China

<sup>b</sup> School of Science, Xi'an University of Architecture and Technology, Xi'an, China

Original scientific paper

<https://doi.org/10.2298/TSCI191112153Z>

*The permeability property of a packed particles material has been caught much attention, it depends upon its pore characteristics caused by the particle accumulation, but the current empirical formulas and the permeable theory could not reveal the effect of the particle accumulation thoroughly. In this paper, a theoretical formula is derived, and the fractal gradation spectrum is adopted to confirm the particle size distribution, furthermore, the pore feature is determined by the particle size and accumulation features, finally a permeability model of the packed particles material is established. In this model, the effect of particle size distribution on pore features is estimated more thoroughly than those in conventional models, and the calculated results are more accurate and verified experimentally.*

**Key words:** particle size distribution, permeability coefficient,  
packed particles material

### Introduction

As one of the most important hydraulic characteristics, the permeability of a packed particles material is an attractive subject for a long time [1-4]. Large numbers of permeability tests were carried out, and various empirical or semi-empirical formulas were generalized [1, 4-7]. Permeability was found closely associated with the particle size distribution in various studies [8-12]. Overall, in current empirical formulas, the effect of particle size distribution (PSD) is usually estimated roughly by simple parameters, but such association has not been investigated thoroughly.

Based on the Kozeny-Carman equation [5], various permeability models were developed [9, 13-15]. Yu and Cheng [16] promoted a fractal permeability model (hereafter referred to as Yu model) for bi-dispersed porous media, which takes into account the pore tortuosity fractal dimension, the pore size fractal dimension and the max pore size. Based on the fractal and capillary features of homogeneous porous media, Xu and Yu [17] established an analytical permeability model (hereafter referred to as Xu model). Both Yu and Xu models considered particle sizes as a 1-D fractal. The packed particle material is essentially characterized by particle features (particle size and accumulation mode), which determine pore features, and the pore features, which determine permeability subsequently. But there are few permeability models so far, which could estimate the effect of such characteristic thoroughly.

In this paper, a theoretical formula of the permeability coefficient is derived, an accurate PSD curve is obtained through the fractal gradation spectrum [18], the pore features were

\* Corresponding author, e-mail: chaoliu@xauat.edu.cn

determined in accordance with the PSD curve, finally the permeability model of the packed particles material is established. The validity of this model is then verified experimentally.

### Permeability coefficient of packed particles material

The packed particles material could be equivalent to an accumulation of permeable cells. Just one permeable pore is assumed in a permeable cell, the pore diameter is  $\lambda$ , the cell side length,  $L_{eq}(\lambda)$ , the cell area,  $S(\lambda)$ , the tortuous length of pore,  $L_t(\lambda)$ , and the porosity  $\phi$ . The number of cells with pore diameter,  $\lambda$ , is  $N(\lambda)$ , correspondingly, the number of pores with the pore diameter  $\lambda$ , is also  $N(\lambda)$ .

According to Hagen-Poiseuille's Law, the flow rate through a single permeable pore is:

$$q(\lambda) = \frac{\pi}{128} \frac{\Delta P}{\mu} \frac{\lambda^4}{L_t(\lambda)} \quad (1)$$

where  $\Delta P$  is the pressure gap and  $\mu$  – the liquid viscosity. For liquid water,  $\mu = 1000 \cdot 10^{-9}$  Ns/mm<sup>2</sup>. The tortuous length of a permeable cell with porosity,  $\phi$ , is [9]:

$$L_t(\lambda) = \tau_{av}(\phi) L_{eq}(\lambda) = (1 - 0.41 \ln \phi) L_{eq}(\lambda) \quad (2)$$

the total flow rate of all the permeable cells is:

$$Q = \sum_{\lambda_{\min}}^{\lambda_{\max}} q(\lambda) N(\lambda) = \frac{\pi}{128} \frac{\Delta P}{\mu} \sum_{\lambda_{\min}}^{\lambda_{\max}} \frac{\lambda^4}{L_t(\lambda)} N(\lambda) \quad (3)$$

The unit flow rate is obtained by unitizing the total flow:

$$Q_{el} = \frac{Q}{\sum_{\lambda_{\min}}^{\lambda_{\max}} N(\lambda)} = \frac{\pi}{128} \frac{\Delta P}{\mu} \frac{\sum_{\lambda_{\min}}^{\lambda_{\max}} f(\lambda)}{\sum_{\lambda_{\min}}^{\lambda_{\max}} N(\lambda)}, \quad f(\lambda) = \frac{\lambda^4}{L_t(\lambda)} N(\lambda) \quad (4)$$

According to Darcy's Law, the permeability could be expressed:

$$K = \frac{\mu L_{eq} Q_{el}}{\Delta P S} = \frac{\pi}{128} \frac{L_{eq}}{S} \frac{\sum_{\lambda_{\min}}^{\lambda_{\max}} f(\lambda)}{\sum_{\lambda_{\min}}^{\lambda_{\max}} N(\lambda)} \quad (5)$$

where  $L_{eq}$  and  $S$  are, respectively:

$$L_{eq} = \frac{\sum_{\lambda_{\min}}^{\lambda_{\max}} L_{eq}(\lambda) N(\lambda)}{\sum_{\lambda_{\min}}^{\lambda_{\max}} N(\lambda)}, \quad S = \frac{\sum_{\lambda_{\min}}^{\lambda_{\max}} S(\lambda) N(\lambda)}{\sum_{\lambda_{\min}}^{\lambda_{\max}} N(\lambda)} \quad (6)$$

The permeability coefficient could be obtained:

$$k = \frac{K\gamma}{\mu} \quad (7)$$

where  $\gamma$  is the liquid bulk density and  $\mu$  – the liquid viscosity. For water,  $\gamma = 9.8 \cdot 10^{-6} \text{ N/mm}^3$ .

### A new permeability model of the packed particles material

#### Basic assumptions

In this paper, particles are projected from a 3-D space to a 2-D plane, subsequently the total permeability of the packed particles material would be represented by the 2-D permeability. Due to the dimension reduction, the particle mass is substituted by the particle area.

Considering the crucial effect of the particle accumulation, the particle clusters are set to be basic permeability cells. Two types of clusters are assumed in this paper, *i.e.*, the type 31 cluster and the type 30 cluster, respectively, as shown in fig. 1. In the type 31 cluster, the bigger particles are called as the skeleton particles, the smaller particles in the center are called as the filling particles. The sizes of all the skeleton particles in the same cluster are assumed to be equal.

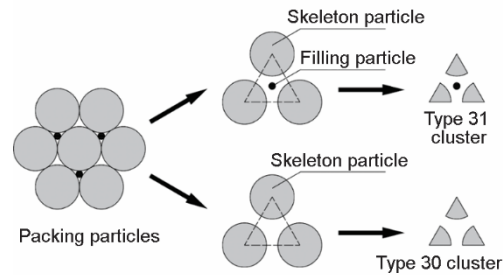


Figure 1. Particle clusters

#### The particle cluster

The type 31 and 30 clusters are shown in fig. 2, where  $R$  is the radius of the skeleton particle,  $r$  – the radius of the filling particle,  $\Delta L_{\max}$  and  $\Delta L$  are expressed in fig. 2. The subscripts of 30 and 31 represent the cluster types.

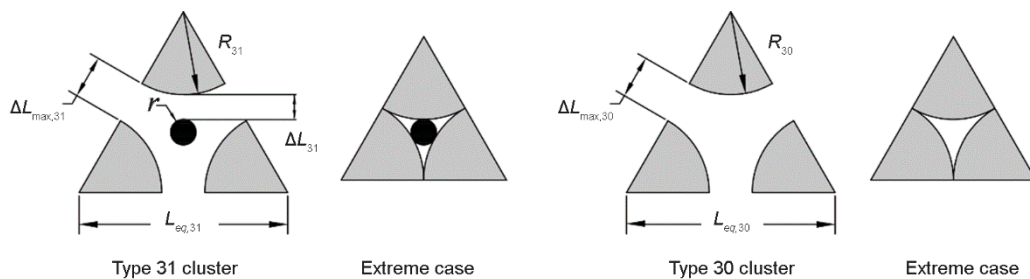


Figure 2. Type 31 and 30 cluster

In an extreme case, a rather low porosity would lead to a rather low permeability. It is reasonable to consider that  $\Delta L_{\max,31} = 0$  in this case, there would be:

$$r = pR_{31}, \quad p = \frac{2}{\sqrt{3}} - 1 \quad (8)$$

It is necessary to hold eq. (8) to guarantee the extreme case. According to the geometric characteristic, key parameters of 31 and 30 cluster types are shown in tab. 2.

**Particle sizes in clusters**

To simplify the calculation of particle content within an arbitrary range, the fractal gradation spectrum [18] is introduced instead of the gradation curve.

**Table 2. Key parameters of cluster**

Parameter	Expression	Parameter meaning
$S_{el}$	$S_{el} = \sqrt{3}(R + 0.5\Delta L_{\max})^2$	The area of cluster
$L_{eq}$	$L_{eq} = 2R + \Delta L_{\max}$	Equivalent side length
$S_{\varphi,el}$	$S_{\varphi,el,31} = S_{el,31} - \frac{\pi}{2}R_{31}^2 - \pi r^2$ $S_{\varphi,el,30} = S_{el,30} - 0.5\pi R_{30}^2$	Pore area
$\varphi$	$\varphi = \frac{S_{\varphi,el}}{S_{el}}$	Porosity
$\Delta L_{31}$	$\Delta L_{31} = \frac{2}{\sqrt{3}}(R_{31} + 0.5\Delta L_{\max,31}) - R_{31} - r$	Distance between skeleton cluster and filling cluster
$\lambda$	$\lambda_{31} = \sqrt{\frac{S_{\varphi,el,31}}{\pi}} - r, \quad \lambda_{30} = \sqrt{\frac{S_{\varphi,el,30}}{\pi}}$	Equivalent wide of pore
$S_{el,ske}$	$S_{el,ske} = 0.5\pi R^2$	Area of skeleton particles in a single cluster
$N$	$N = \frac{S_{ske}}{S_{el,ske}}$	The number of clusters

**Fractal gradation spectrum**

A gradation could be comprised of two gradations with fractal characteristics:

$$M_T = \sum_{i=1}^n M_{Ti}, \quad n = 2 \quad (9a)$$

$$M_i(R) = M_{Ti} \left( \frac{R}{R_{Ti}} \right)^{3-D_i} \quad \text{when } R = R_{Ti} \quad i = 1, 2 \quad (9b)$$

$$M_i(R) = M_{Ti} \quad \text{when } R \geq R_{Ti}$$

where  $M_T$  is the total mass of all particles,  $M_{Ti}$  – the total mass of particles corresponding to the  $i^{\text{th}}$  gradation,  $R$  – the particle radius,  $R_{Ti}$  – the maximum particle size corresponding to the  $i^{\text{th}}$  gradation,  $M_i(R)$  – the total mass less of particles with the radius less than  $R$  for the  $i^{\text{th}}$  gradation, and  $n$  – the number of gradations. The regression target function is achieved by the least-squares method:

$$F_{obj} = \sum_{j=1}^m \left\{ \log \left[ \sum_{i=1}^n M_i(R_j) \right] - \log[M_T P(R_j)] \right\} \quad (10)$$

### Cluster particle group

All the particles with radius  $R$  and  $r = pR_{31} = pR$ , in section *The particle cluster*, are put in a group, named as the cluster particle group. Particles in a gradation could be distributed into several cluster particle groups. It is assumed that, clusters could only be formed by particles within the same cluster particle group, and the mean porosity of clusters formed within a same cluster particle group is equal to the overall porosity  $\varphi_0$ . Considering simplicity of calculation, it is suggested to select several cluster particle groups as representatives of actual particle sizes for calculation.

The radius of the skeleton particle in the  $i^{\text{th}}$  cluster particle group is denoted as  $R_i$ . There is:

$$R_i = \delta^{i-1} R_{\max} \quad (11a)$$

$$\min(R_i) = R_{cr} \quad (11b)$$

where  $\delta$  is determined according to original particle size features, it is comprehensive that  $0 < \delta < 1$ . The  $R_{cr}$  is the minimum skeleton particle size in calculation, which is determined in section *Minimum skeleton particle size*.

### Minimum skeleton particle size

Piping is common in the permeable behavior of packed particles materials, that is, fine grains would move or be washed away by the flow along pore channels [4]. These fine grains could not participate in forming permeable cells. Consequently, particle sizes in least permeability cells depend on particles lost in piping. According to [4],  $d_{10}$  is the maximum size of particles lost in piping. Therefore,  $d_{10}$  is suggested to be the minimum skeleton particle size. According to eq. (9), there is:

$$\sum_{i=1}^n M_i(R_{cr}) = 10\% M_T \quad (12)$$

where  $R_{cr}$  could be obtained by solving eq. (12). Additional cases of adopting  $d_9$  and  $d_{11}$  as the minimum skeleton particle size were discussed in section *Verification and discussion*.

According to eqs. (11) and (12), particle sizes adopted in calculation could be determined. Combined with eq. (9), with a given  $M_T$ , the mass of particles adopted could be solved, its area could be determined simultaneously for the 2-D case. With ascertained particle sizes and areas, parameters of clusters could be confirmed by eqs. (1)-(7).

### Equivalent pore size

The uniaxial permeation in 31 and 30 cluster types is shown in fig. 3, related pore diameters include  $\Delta L_{\max,31}$ ,  $\Delta L_{31}$ ,  $\Delta L_{31}$ ,  $\Delta L_{\max,30}$ , and  $\Delta L_{30}$ .

Considering the non-homogeneity of the particle accumulation and a possible turbulent flow in permeation, the equivalent permeable pore size is assumed based on physical meaning. The maximum, intermediate, and minimum pore sizes are shown in tab. 3, corresponding to upper, middle, and lower values of permeability coefficient respectively.

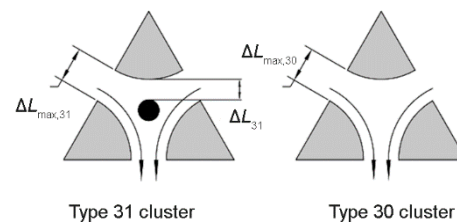


**Figure 3. Uniaxial permeation in type 31 and 30 cluster**

**Table 3. Equivalent permeable pore size**

Pore size	Type 31 cluster	Type 30 cluster
$\lambda_{\max}$	$2\max(\lambda_{31}, \Delta L_{31}, \Delta L_{\max,31})$	$2\max(\lambda_{30}, \Delta L_{\max,30})$
$\lambda_{\text{middle}}$	$\min(\lambda_{31}, \Delta L_{31}, \Delta L_{\max,31}) + \max(\lambda_{31}, \Delta L_{31}, \Delta L_{\max,31})$	$\min(\lambda_{30}, \Delta L_{\max,30}) + \max(\lambda_{30}, \Delta L_{\max,31})$
$\lambda_{\min}$	$2\min(\lambda_{31}, \Delta L_{31}, \Delta L_{\max,31})$	$2\min(\lambda_{30}, \Delta L_{\max,30})$

According to tab. 2,  $\Delta L_{31}$  and  $\lambda_{31}$  are expressions of  $\Delta L_{\max,31}$ ,  $\lambda_{30}$ , and  $\Delta L_{\max,30}$ . Therefore,  $\Delta L_{\max,31}$  and  $\Delta L_{\max,30}$  are only needed in our theoretical analysis. As is assumed in section *Cluster particle group*, clusters could only be formed by particles within a same cluster particle group, there might be two cases:

- the skeleton particle size of 31 and 30 cluster types are both  $R$ , i.e.  $R_{31} = R_{30} = R$  and
- the skeleton particle size of 31 cluster type is  $R$ , that of 30 cluster type is  $r$ ,  $R_{31} = R$ ,  $R_{30} = r = pR$ .

In order to solve  $\Delta L_{\max,31}$  and  $\Delta L_{\max,30}$ , assumptions are introduced:

$$\Delta L_{\max,31} = \eta R_{31}, \quad \Delta L_{\max,30} = \eta R_{30} \quad (13)$$

Key expressions based on such assumptions are shown in tab. 4.

**Table 4. Key expressions**

Expression	Case1	Case2
$\eta$	–	$2\sqrt{\frac{S_{ske,30} + S_{ske,31}(1+2p^2)}{S_{ske,30} + S_{ske,31}}} \frac{0.5\pi}{\sqrt{3}(1-\phi_0)} - 2$
$\Delta L_{\max,31}$	$\sqrt{\frac{S_{el}}{3}} - 2R$	$\eta R$
$\Delta L_{\max,30}$	$\sqrt{\frac{S_{el}}{3}} - 2R$	$\eta pR$
$\lambda_{31}$	$\sqrt{\frac{\sqrt{3}(R + 0.5\Delta L_{\max,31})^2 - 0.5\pi(1+2p^2)R^2}{\pi}} - pR$	$\sqrt{\frac{\sqrt{3}(R + 0.5\Delta L_{\max,31})^2 - 0.5\pi(1+2p^2)R^2}{\pi}} - pR$
$\lambda_{30}$	$(R + 0.5\Delta L_{\max,30})\sqrt{\frac{\sqrt{3}}{\pi}}$	$(R + 0.5\Delta L_{\max,30})\sqrt{\frac{\sqrt{3}}{\pi}}$
$\Delta L_{31}$	$2\sqrt{\frac{S_{el}}{3\sqrt{3}}} - (1+p)R$	$\left(\frac{2+\eta}{\sqrt{3}} - 1 - p\right)R$

Note:  $S_{el}$  is the area of permeable cell and  $S_{ske}$  – the area of skeleton articles.

## Verification and discussion

### Verification

Considering applicable conditions of Darcy's Law, eight groups of test data of low porosity materials [19] were adopted for verification. Test material is meso-micro weathered

sandstone, porosities of all the test groups are the same 10.8%. The  $\delta$  was set to be 0.5 based on particle sizes. Due to the consistency of porosity, influence of PSD on permeability could be better reflected.

Calculated results of the model in this paper are shown in fig. 4, P5 (content of grains with diameter less than 5 mm) was taken as the  $x$ -axis. Additional calculated results of Kozeny-Carman equation [5], Yu model [16], and Xu model [17] were also shown for comparison.

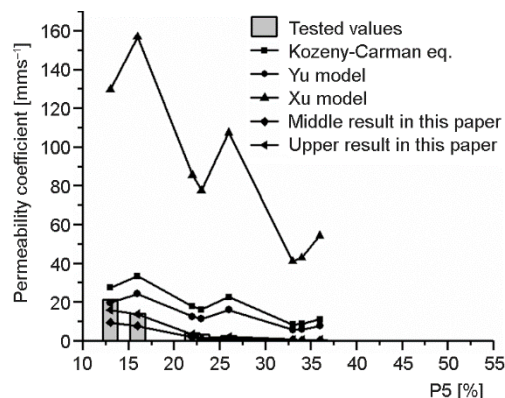


Figure 4. Calculated results

## Discussion

### Effect of fine aggregate content

The P5 is inversely proportional to the critical velocity in [19]. When P5 is lower than 30%, the calculated results adopting  $\lambda_{\max}$  would be closer to tested values, fig. 5(a). When P5 is higher than 30%, we adopted  $\lambda_{\text{middle}}$ , fig. 5(b). This phenomenon is associated with the filling effect of fine aggregate. The higher fine aggregate content P5, the more adequate filling effect on the permeable pores, thus the smaller permeable pore size, finally the lower critical velocity and permeability.

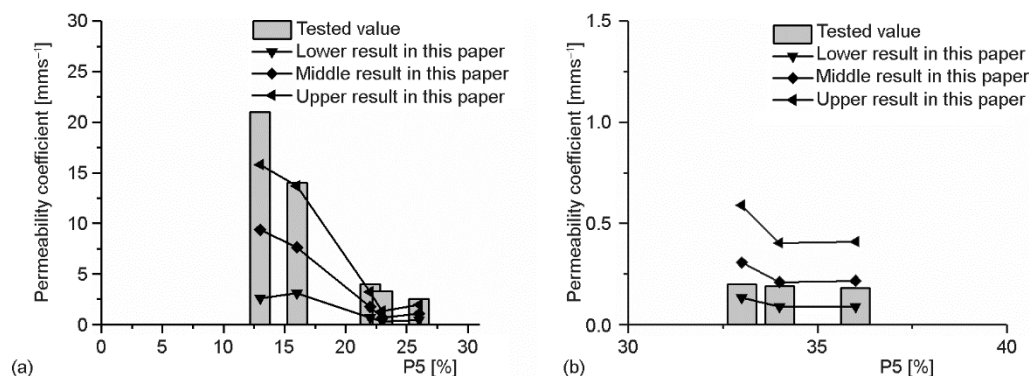


Figure 5. Calculated results adopted different equivalent pore size

### Effect of minimum particle size

Calculated results with the minimal particle sizes of  $d_9$ ,  $d_{10}$ , and  $d_{11}$ , respectively are shown in fig. 6. Positive association is notable between the permeability coefficient and the minimum particle size. This phenomenon is comprehensive according to the piping mechanism. In the determination of the minimum particle size, the higher content of finer particles is set, the more fine-particle lost in piping, and the larger minimum particle size is adopted.

## Conclusion

In this paper, test and theoretical studies on permeability of the packed particle material were reviewed, a new permeability model was established. The 2-D fractal spectrum was

adopted to estimate PSD, the effect of PSD on pore features was more adequate through permeable cells formation. Combined with Hagen-Poiseuille's Law and Darcy's Law, the

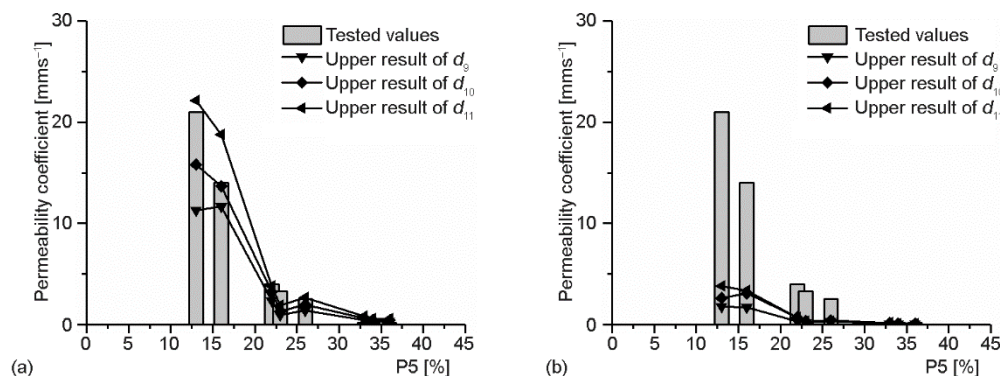


Figure 6. Minimum particle size vs. calculated permeability

permeability coefficient could be obtained. The validity of this model was verified through the test data. The accuracy of this model is significantly higher than those of the conventional formula and models.

Compared with conventional formulas and models, this suggested model, with small computation and clear physical meaning, reflected the influence of PSD on permeability effectively and thoroughly. In addition, this model could provide theoretical tool for an accurate seepage simulation, and theoretical support for a seepage failure analysis and a seepage control design.

This model is suitable for the packed particle material for Darcy percolation and Newton flow. Further studies would be extended to non-Darcy flow and non-Newtonian fluids.

### Acknowledgment

The authors would like to acknowledge the financial support provided to this study by the National Natural Science Foundation of China (Grant No. 51878546), the Innovative Talent Promotion Plan of Shaanxi Province (Grant No. 2018KJXX-056), the Key Research and Development Projects of Shaanxi Province (Grant No. 2018ZDCXL-SF-03-03-02), the Science and Technology Innovation Base of Shaanxi Province (Grant N0. 2017KTPT-19) and the Outstanding Youth Science Foundation Project of Shaanxi Province (2020JC-46).

### References

- [1] Terzaghi, K., et al., *Soil Mechanics in Engineering Practice*, John Wiley & Sons, New York, USA, 1996
- [2] Jie, L., *Soil Seepage Stability and Seepage Control* (in Chinese), Water Resources and Electric Power Press, Beijing, China, 1992
- [3] Jie, L., *Seepage Control of Earth-Rock Dams Theoretical Basis, Engineering Experiences and Lessons* (in Chinese), China Waterpower Press, Beijing, China, 2005
- [4] Changxi, M., *Seepage Computation Analysis & Control* (in Chinese), Water Resources and Electric Power Press, Beijing, China, 1990
- [5] Carman, P. C., Fluid Flow through Granular Beds, *Trans. Inst. Chem. Eng.*, 15 (1937), pp. 150-166
- [6] Liu, J., Experimental Study of Optimum Gradation of Crushed Stone Cushion for Concrete-Face Rockfill Dam, *Hydro-Science Engineering*, 4 (2001), pp. 1-7
- [7] Pape, H., et al., Permeability Prediction for Low Porosity Rocks by Mobile NMR, *Pure Applied Geophysics*, 166 (2009), 5, pp. 1125-1163



- [8] Lijun, S., et al., Investigation on Permeability of Sands with Different Particle Sizes (in Chinese), *Rock and Soil Mechanics*, 35 (2014), 5, pp. 1289-1294
- [9] Xiao, B., et al., A Fractal Model for Kozeny-Carman Constant and Dimensionless Permeability of Fibrous Porous Media with Roughened Surfaces, *Fractals*, 27 (2019), 7, ID 1950116
- [10] Shao, S., et al., Pore Characteristics of Coarse Grained Soil and their Effect on Slurry Permeability (in Chinese), *Chinese Journal of Geotechnical Engineering*, 31 (2009), 1, pp. 59-65
- [11] Arya, L. M., Paris, J. F., A Physicoempirical Model to Predict the Soil Moisture Characteristic from Particle-Size Distribution and Bulk Density Data, *Soil Science Society of America Journal*, 45 (1981), 6, pp. 1023-1030
- [12] Shepherd, R. G., Correlations of Permeability and Grain Size, *Groundwater*, 27 (1989), 5, pp. 633-638
- [13] Goktepe, A. B., Sezer, A., Effect of Particle Shape on Density and Permeability of Sands, *Proceedings of the Institution of Civil Engineers-Geotechnical Engineering*, 163 (2010), 6, pp. 307-320
- [14] Xiao, B., et al., A Novel Fractal Solution for Permeability and Kozeny-Carman Constant of Fibrous Porous Media Made up of Solid Particles and Porous Fibers, *Powder Technology*, 349 (2019), May, pp. 92-98
- [15] Valdes-Parada, F. J., et al., Validity of the Permeability Carman-Kozeny Equation: a Volume Averaging Approach, *Physica A: Statistical Mechanics & its Applications*, 388 (2009), 6, pp. 789-798
- [16] Yu, B., Cheng, P., A Fractal Permeability Model for Bi-Dispersed Porous Media, *International Journal of Heat Mass Transfer*, 45 (2002), 14, pp. 2983-2993
- [17] Xu, P., Yu, B., Developing a New Form of Permeability and Kozeny-Carman Constant for Homogeneous Porous Media by Means of Fractal Geometry, *Advances in Water Resources*, 31 (2008), 1, pp. 74-81
- [18] Liu, X., et al., Relationship between Physical Properties and Particle-Size Distribution of Geomaterials, *Construction Building Materials*, 222 (2019), Oct., pp. 312-318
- [19] Qiu, X.-D., et al., Effect of Particle-Size Characteristics on Seepage Property of Rockfill (in Chinese), *Rock Soil Mechanics-Wuhan*, 25 (2004), June, pp. 950-954